International Journal of Food Science +Technology

International Journal of Food Science and Technology 2021, **56**, 1641–1648

Original article

Acid-induced aggregation and gelation of heat-treated chia proteins

Débora N. López,[1,2,3*] Romina Ingrassia,[1,2,4] Pablo Busti,[1] Jorge Wagner,[5] Valeria Boeris[1,2,3] & Darío Spelzini[1,2,3]

1 Facultad de Ciencias Bioquímicas y Farmacéuticas, Universidad Nacional de Rosario (UNR), Suipacha 531, Rosario, Argentina
2 CONICET, Bv. 27 de Febrero 210, Rosario, Argentina
3 Facultad de Química e Ingeniería del Rosario, Pontificia Universidad Católica Argentina (UCA), Pellegrini 3314, Rosario, Argentina
4 Facultad de Ciencias Veterinarias, UNR, Ovidio Lagos y Ruta 33, Casilda, Argentina
5 Departamento de Ciencia y Tecnología – CONICET, Universidad Nacional de Quilmes, Roque Sáenz Peña 352, Bernal, Buenos Aires B1876BXD, Argentina

(Received 3 April 2020; Accepted in revised form 9 September 2020)

Summary This work studied for the first time the acid-induced aggregation and gelation of heat-treated chia protein isolates obtained by extraction at pH 10 or 12 (CPI10 and CPI12, respectively). The aggregation state of proteins was modified during acidification. The size of the aggregates was reduced for both samples when the pH decreased but below pH 4.5 further protein aggregation took place for CPI12. Gelation of CPI12 was completed after about 30 min of acidification with glucone-δ-lactone. By contrast, this period was not enough to reach a constant value in G' for CPI10. When gelation was ensured, confocal laser scanning micrographs from those gels revealed a coarse and irregular structure with large pores (median size of diameters: 30 μm). Instead, micrographs from CPI12 cold gels showed a more regular and interconnected network, with smaller pores (median size of diameters: 9 μm). These differences are consistent with a higher elastic behaviour (G'_{max} = 13.6 ± 0.1 Pa).

Keywords Acidified systems, cold-set gelation, glucone-δ-lactone, *Salvia hispanica* L.

Introduction

In recent years, there has been a growing interest in the development of gels formed from plant proteins or their mixture with milk proteins (Mäkinen *et al.*, 2015). Gels from protein suspensions may be formed by thermal (Mir *et al.*, 2019) or high-pressure (Li *et al.*, 2018) treatments, covalent crosslinking by transglutaminase (Djoullah *et al.*, 2015; Cui *et al.*, 2019), or due to a decrease in the colloidal stability of denatured protein suspensions by divalent cation addition (Chu *et al.*, 2019) or pH-shifting (Jiang *et al.*, 2017). Ultrasonic treatments (Gharibzahedi & Smith, 2020) and the combination of different type of proteins (Cui *et al.*, 2019) or proteins/polysaccharides mixtures (Chu *et al.*, 2019) are also known to improve gel characteristics.

Sample composition and many factors related to the media affect the acid-induced gelling process of heat-treated proteins and the properties of the gels. If more than one sample is being assayed, it is not always possible to equal both the composition and the medium conditions. Thereby, some authors prefer to standardise soluble protein concentration (Lu *et al.*, 2017) whereas others use the same amount of dispersed sample (Soukoulis *et al.*, 2019). In some cases, the pH of the heat-treated samples is adjusted before acidification (Kharlamova *et al.*, 2018), whereas in others, the pH at the beginning of acidification is a consequence of the differences among samples (Donato *et al.*, 2011). Thus, the selection of the experimental conditions assayed is frequently related to the aim of the study.

Since the mechanical properties are one of the most important characteristics of gels, rheological tests are generally carried out. Besides, image analysis of gel´s micrographs is frequently reported since it brings information about gel´s microstructure (Donato *et al.*, 2011; Kharlamova *et al.*, 2018). In addition, protein solubility, the size of the protein aggregates and the least amount of sample required for gelation are often determined (Donato *et al.*, 2011; Djoullah *et al.*, 2015; Mäkinen *et al.*, 2015; Mishyna *et al.*, 2019).

Nowadays, chia seeds are among the most widely consumed seeds because of their well-known nutritional quality (López *et al.*, 2018). One strategy to get value out of the by-product obtained after the

*Correspondent: E-mail: dlopez@fbioyf.unr.edu.ar

doi:10.1111/ijfs.14784

extraction of oil is to use it as a raw material to concentrate proteins, which are particularly attractive from a nutritional point of view (López *et al*., 2018). In a previous study, we reported the isolation of chia proteins from this by-product through alkaline extraction followed by isoelectric precipitation, attaining high recovery yields. Chia protein isolates (CPI) were obtained by extraction at pH 10 or 12. The electrophoretic pattern under reducing conditions of these proteins showed the presence of globulin and albumin fractions. Despite their different techno-functional properties, both CPI revealed a promising use in the food industry (López *et al*., 2018). Thus, this work studies for the first time the acid-induced aggregation and gelation of heat-treated CPI, focusing on the effect of the extraction conditions.

Materials and methods

Materials

Milled and defatted chia grains were purchased from Sturla S.R.L. (Buenos Aires, Argentina). All the chemicals used were of analytical grade.

Preparation of chia protein isolates

CPI were prepared through isoelectric precipitation at two different extraction pH, 10.0 and 12.0 (López *et al*., 2018). Briefly, milled and defatted chia seeds were hydrated with distilled water (ratio 1:20), stirred for 30 min and centrifuged at 10 000***g*** for 15 min. After centrifugation, the mucilage concentrated in an intermediate phase was carefully removed. The upper phase and the precipitate were mixed, and the resulting slurry was adjusted at pH 10.0 or 12.0 with alkali and stirred for 1 h. The supernatant obtained by centrifugation at 10 000***g*** for 15 min was acidified to pH 4.5, while this slurry was kept stirring for 1 h to ensure the precipitation of chia proteins. Proteins were recovered by another centrifugation step, and pellets were dispersed in diluted alkali adjusted to pH 10.0 or 12.0, depending on their extraction pH. Samples were freeze-dried and labelled as CPI10 or CPI12, respectively. Three independent samples were obtained for each one of the isolation procedures carried out.

Physicochemical characterisation of the CPI and their suspensions

The ash content of both CPI (Mortensen & Wallin, 1989) and the content of total dietary fibre (TDF) were determined (Prosky *et al*., 1985; Table S1).

Suspensions of CPI were prepared by dissolution in distilled water at a proper concentration and stirred for 30 min at 20 °C. Suspension was heated for 5 min at 100 °C and then cooled down for 10 min at 0 °C. Afterwards, they were left at 20 °C for 1 h. These suspensions were named as heat-treated samples. The pH of these samples was determined. The protein solubility of the heat-treated samples was determined by the bicinchoninic acid assay method (Smith *et al*., 1985).

Determination of the minimum amount of sample required for gel formation

Heat-treated suspensions of CPI (concentrations: 1, 2, 3, 4, 5, 6, 7, 8, 9, 10, 12, 14, 16, 18, 20, 25 and 30 g L^{-1}) were acidified at 20 °C by the addition of glucone-δ-lactone (GDL) at the same concentration at which each sample was dissolved. Systems were incubated for 24 h, and gel formation was determined by turning the tubes upside down.

Acid-induced aggregation

CPI10 and CPI12 were dispersed in distilled water at 0.1 g L^{-1} and stirred for 30 min. Heat-treated suspensions were acidified at 20 °C by the addition of GDL (0.1 g L^{-1}). The time course of the average size of particles during acidification was studied through the dependence of turbidity (τ) on the wavelength (λ) (Risso *et al*., 2007). The absorption spectra were obtained every minute during acidification in the 400–600 nm range, using a Spekol 1200 spectrophotometer (Analytik Jena AG, Jena, Germany). The aggregation process of both CPI was studied through the β parameter, which is related to the average size of the soluble particles (Risso *et al*., 2007). The β parameter was calculated from the slope of log τ vs log λ plots, as follows:

$$\beta = 4.2 + \delta\log\tau/\delta\log\lambda \quad (1)$$

Acid-induced gelation

Aqueous dispersions of both CPI (30 g L^{-1}) were stirred for 30 min before heat treatment. Afterwards, heat-treated samples were acidified at 20 °C by the addition of GDL (15 g L^{-1}). Rheological changes during gelation were studied using a controlled stress rheometer AR-G2 (TA Instruments, New Castle, USA), equipped with a 40 mm diameter stainless-steel plate geometry (gap of 1 mm). Gel formation was monitored at 20 °C by measuring the storage (G') and loss (G'') moduli after the addition of GDL. Oscillation stress and frequency were fixed at 0.1 Pa and 0.1 Hz, respectively. G' and G'' values were registered every 20 s. pH was also measured during acidification. The time and pH at which the crossover between G' and G'' took place were defined as t_{gel} and pH_{gel}, respectively. The acidification kinetics due to GDL

hydrolysis was fitted to a first-order kinetic model (Table S2).

When equilibrium was reached, frequency sweep measurements were carried out at 20 °C. Oscillation stress was fixed at 0.1 Pa, whereas frequency varied from 0.1 to 10 Hz.

Microstructure of chia protein acid-induced gels

Three millilitres of aqueous dispersions of both CPI was prepared in distilled water at a concentration of 30 g L^{-1} and was stained with 20 μL of 0.02 g L^{-1} Rhodamine B before heat treatment. Images of the heat-treated samples and the systems obtained after acidification with GDL (15 g L^{-1}) for 2 h were obtained by using a confocal laser scanning microscope (CLSM) (Nikon Eclipse TE-2000-E) with an oil immersion objective of 60×. The excitation wavelength was 488 nm, whereas the emission wavelength was 568 nm. The size distribution of pores and protein aggregates of each sample (Lombardi *et al*., 2018), and two textural features, entropy and contrast, were determined (Shih *et al*., 2013).

Statistical analysis

Determinations were made at least in duplicate. The effect of the extraction conditions on the gelling ability of chia proteins was analysed through *t*-tests. Data were verified to make sure they fit the normal distribution and homogeneity of variance before performing parametric tests. When the *P*-values (*P*) were lower than 0.05, the differences were considered significant.

Results and discussion

Physicochemical characterisation of the CPI and their heat-treated dispersions

CPI12 showed a lower content of TDF than CPI10 ($P = 0.003$) whereas a higher content of ash ($P < 0.001$), this latest related to its higher solubilisation pH. Heat-treated dispersions showed different pH ($P < 0.001$), also related to the different extraction procedures. After heat treatment, the soluble proteins concentration was higher in CPI10 than in CPI12 (Table S1), same as for the dispersions without heat treatment (López *et al*., 2018). The insoluble protein after heat treatment represents 9% of the total protein content for CPI10 and 31% for CPI12.

Determination of the minimum amount of sample required for gel formation

The minimal amount of dispersed sample required for gel formation was significantly different between both CPI ($P = 0.008$). Results obtained (Table S1) are in the same range as those reported for the acid-induced gelation of whey proteins (Alting *et al*., 2000) but smaller than those required for quinoa protein isolates (Montellano Duran *et al*., 2018). By contrast, a greater amount of sample was required for thermal induced gels of honey bee brood soluble proteins (Mishyna *et al*., 2019), high-pressure induced gels from β-lactoglobulin (Li *et al*., 2018) or gels obtained by transglutaminase crosslinking of pea albumin and globulins (Djoullah *et al*., 2015).

Although the content of crude protein and the protein solubility is higher in CPI10 than in CPI12, this may not be the determining factor in the gelling ability of these samples.

Acid-induced aggregation

Figure 1 shows the variation of the β parameter over pH during the acidification process of both CPI. Variations in β parameter may be interpreted in terms of variations in size of the soluble particles.

Before the addition of GDL, the β value of the soluble particles after heat treatment of CPI10 was considerably higher than that for CPI12. Thus, the higher concentration of solubilised proteins in CPI10 may have induced greater association among particles, leading to larger clusters.

Both samples also showed significant differences during acidification. For CPI10, the β value remained almost constant at first, until pH = 4.3, at which it dropped abruptly. This decrease in the β value indicates a decrease in the average size of the soluble aggregates due to acidification. For CPI12, the β value reached a minimum at pH = 4.6, after which it increased and remained nearly constant. This behaviour has already been reported for the acid-induced aggregation of sodium caseinate (Hidalgo *et al*., 2015) and quinoa proteins (Montellano Duran *et al*., 2018), suggesting the formation of larger protein aggregates by the association among particles due to the lack of electrostatic repulsion. Since CPI10 showed no further increase in the β value, soluble aggregates formed from this sample were not able to restructure to form larger aggregates in the period of time analysed.

Acid-induced gelation

The kinetics of GDL hydrolysis is shown in Fig. 2. The acidification process did not fit properly to a single exponential decay model, suggesting that the sol-gel transition of chia proteins influenced the GDL hydrolysis rate. This was also observed during the gelation process of whey proteins (Soukoulis *et al*., 2019). The data obtained fitted a first-order kinetic model. The decay constants k_1 ($P = 0.0344$) and k_2 ($P = 0.0263$;

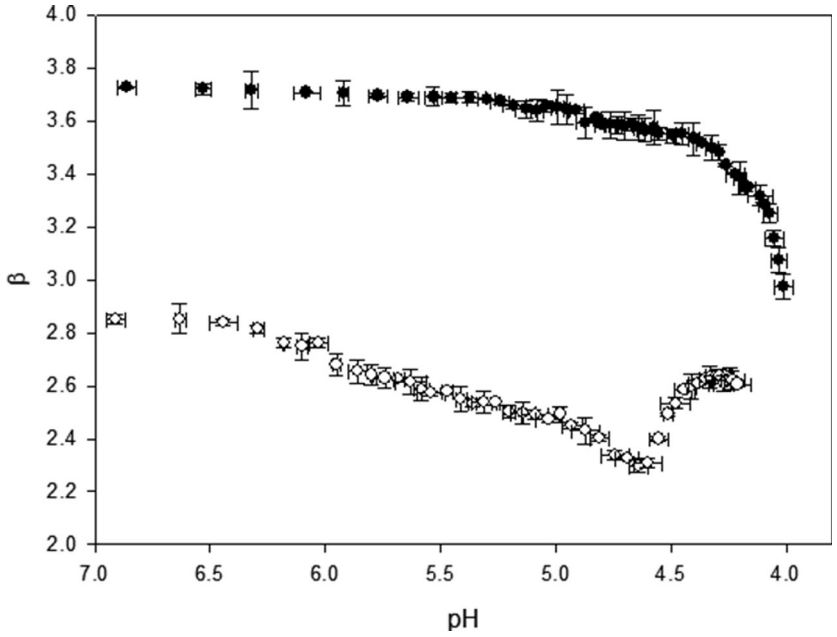

Figure 1 Dependence of the β parameter over pH during the acidification process of CPI10 (black symbols) and CPI12 (white symbols).

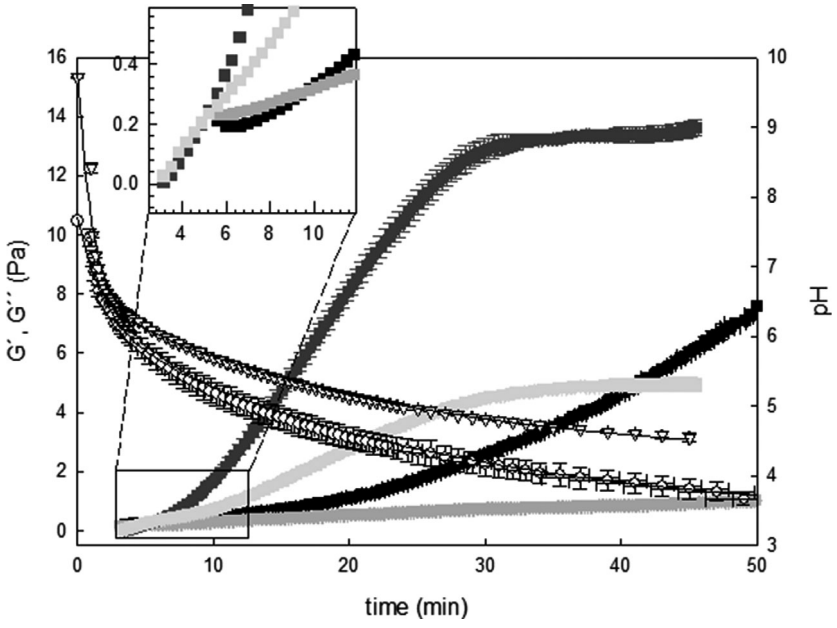

Figure 2 Development of the storage (G') modulus, loss (G'') modulus and pH during the acid-induced gelation of CPI10 and CPI12. G' (■), G'' (□) and pH (○) for CP10 and G' (■), G'' (□) and pH (△) for CP12. Lines represent the variation pH fitted to a first-order equation: $pH = pH_\infty + a \exp(-k_1 t) + b \exp(-k_2 t)$.

Table S2) were higher for CPI12 than for CPI10. The lower acidification kinetics showed by CPI10 was probably due to the higher content of fibre and proteins, which may be responsible for greater buffering ability.

Rheological behaviour of CPI during acid-induced gelation

CPI heat-treated dispersions showed a similar G' and G'' behaviour upon acidification (Fig. 2). Similar changes in both moduli were also reported for cold-set gel formation of whey proteins (Alting *et al.*, 2003), pea proteins (Mession *et al.*, 2015) and soy flour proteins (Ingrassia *et al.*, 2019). At an early stage, G' and G'' values remained low and the system showed a predominant viscous behaviour, since G' was lower than G''. After some time, G' and G'' suddenly increased, making G' higher than G'', which suggests both a solid-like behaviour and a protein network formation. It was at the beginning of this latter stage that G'

equals G'', which allowed us to determine t_{gel} and pH_{gel} (Table S2). In this case, pH_{gel} indicates that CPI12 proteins present lower electrostatic stability ($P = 0.03$) and are thus more prone to protein aggregation than CPI10 proteins (Hidalgo *et al.*, 2015; Ingrassia *et al.*, 2019). Therefore, CPI12 may present a higher tendency to cold-set gel formation. The fact that G' did not reach a constant value after one hour of gelation of CPI10 probably suggests that the formation of an elastic gel structure is not completed in the period of time analysed.

Mäkinen *et al.* (2015) reported that the denaturation pH during the heat treatment at 100 °C of quinoa protein isolate dispersions significantly influenced the cold gelation properties. These authors reported that heat treatment at a more alkaline pH promoted the formation of cold-set gels with higher G'. These findings may be useful to explain the differences observed in both CPI rheograms.

It is already known that even after 5 days of the addition of GDL, the pH value may continue lowering (Cavallieri & Da Cunha, 2008). Although the pH value slightly decreased, G' value remained constant for CPI12 after 30 min of gelation; thus, we considered that this sample had attained a pseudo-equilibrium stage. The mechanical spectrum of CPI12 acidified systems (Table S2) was consistent with a gel rather than an entanglement network. The observed dependence of G' on ω – a characteristic of weak gels – fitted the power law type (Table S2). The n and tan δ values support the fact that the viscoelastic behaviour of these gels is not mainly elastic (Özkan *et al.*, 2002). The mechanical properties of the gels obtained from CPI10 could not be studied through frequency sweep measurements since G' did not reach a constant value in the period of time analysed.

Microstructure of heat-treated suspensions and gels

The microstructure of both the heat-treated suspensions from CPI10 and CPI12 and that of the acid-induced gels formed was visualised with a CLSM (Fig. 3).

Heat treatment of CPI10 led to protein aggregates whose median size was 2 μm (Fig. 3a). By contrast, micrographs from the heat-treated suspensions of CPI12 (Fig. 3b) did not show an appreciable association among proteins, suggesting that they remained in suspension after heating. These results are consistent

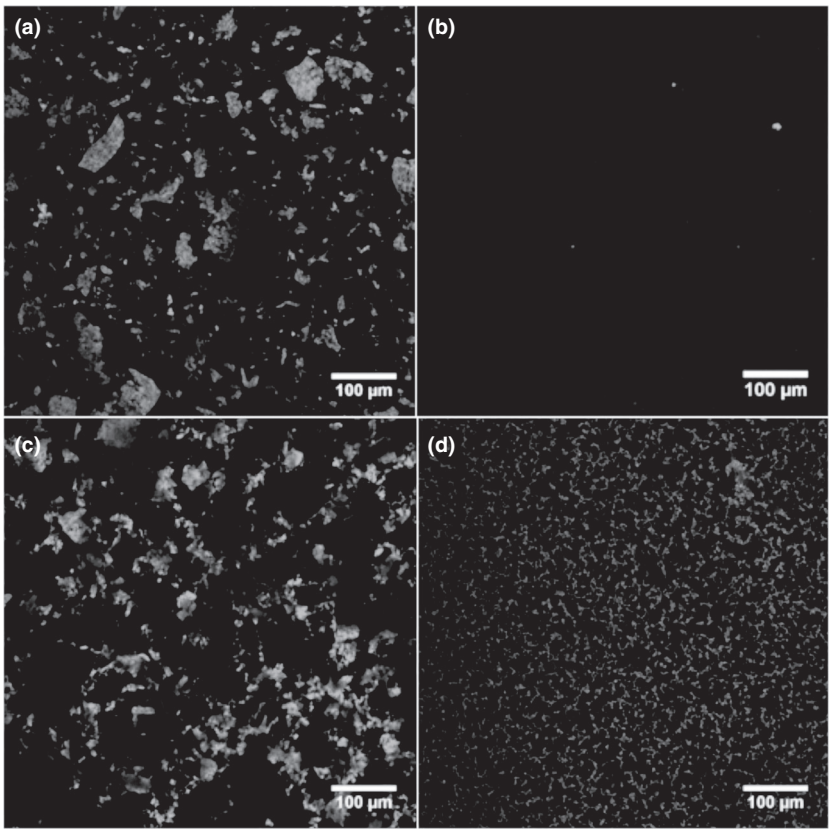

Figure 3 Confocal laser scanning microscopy of heat-treated suspensions of chia protein isolates obtained by extraction at pH 10 and 12 (a and b, respectively). Microstructure of acid-induced gels from CPI10 and CPI12 (c and d, respectively).

with those previously discussed, since the β parameter obtained before GDL addition was significantly higher for CPI10 than for CPI12.

The size of the heat-treated proteins has been closely related to the development of the rheological properties of the gels. According to Mession *et al.* (2015), the presence of macro-aggregates in heat-treated dispersions may be detrimental for gel formation. More precisely, Liu *et al.* (2016) reported the formation of a weakly interconnected protein network from microparticles (between 1 and 10 μm) of whey proteins. By contrast, gelation from nanoparticles (whose size is lower than 1 μm) occurred faster and formed a denser network. The findings obtained in the present work are in the same trend as those described above.

Micrographs from CPI10 cold-set gels (Fig. 3c) showed a similar structure to those of the heat-treated dispersions but with a higher median size of the protein aggregates (Table S3). Conversely, a regular fine structure was observed in the gels from CPI12 (Fig. 3d). A similar behaviour was observed for the cold gelation of quinoa proteins. Samples that were heat-treated at pH 8.5 showed coarse and irregular clusters of aggregated particles after acidification. However, a regular gel system was formed from samples heat-treated at pH 10.5 (Mäkinen *et al.*, 2015). As discussed above, the pH of the heat-treated samples was also significantly different in the present work (Table S1) and may have influenced the gelation properties of both CPI.

The addition of GDL diminished the repulsive forces of the heat-treated CPI10, leading to the formation of coarse aggregates. Therefore, low G' values were obtained throughout the gelation process. When CPI12 was acidified after heat treatment, the soluble aggregates cross-linked to form a regular and fine network with a higher G' (Alting *et al.*, 2004).

Entropy and contrast of the images of the acidified systems were determined (Table S3). Images from CPI12 gels showed higher entropy than images from CPI10 acidified systems, indicating that there is a greater amount of grey-level transitions. On the other hand, contrast was lower for CPI12 images, suggesting that they presented a greater amount of tone variations of high magnitude, that is that CPI10 images showed a more heterogeneous and rougher microstructure (Hernández-Carrión *et al.*, 2015).

High contrast values may be related to low-size particles (Donato *et al.*, 2005); however, heat-treated and acidified CPI10 suspensions presented coarse particles and the contrast of these images was high. This may be explained considering that proteins seem to be concentrated in high-sized particles, remaining an extremely low amount of protein in suspension. In agreement with Shih *et al.* (2013), images obtained from CPI12 gels may be described as more monotone and smooth.

Conclusion

This work describes for the first time the ability of chia proteins to develop acidified systems. Considering our results, the obtainment of CPI through solubilisation at different alkaline pH significantly affected their aggregation and cold-set gelation. The rheological characterisation of the acid-induced gelation is clearly consistent with the results obtained from the study of aggregation, highlighting the relationship between both processes.

As for other proteins studied, protein concentration, pH and the size of the heat-treated aggregates proved to be important factors which determined the rheological properties of the acidified systems from chia proteins. The soluble aggregates formed at the end of the aggregation process for CPI10 were not able to form a regular network, leading to a coarse and irregular structure after acidification. By contrast, CPI12 formed a regular and interconnected gel. In the present work, we found that the modification of the extraction procedure of chia proteins provides an important opportunity for the development of a wide variety of acidified food products with different textures.

Acknowledgments

Professors from English Department of Facultad de Ciencias Bioquímicas y Farmacéuticas, UNR, have revised the article. DNL and RI were granted by CONICET. This work was supported by grants from ANPCyT (PICT 2017-0937 and PICT 2018-02872) and from UNR (80020190100129UR and 80020180300 078UR). The authors have no conflict of interest to declare.

Ethics approval

Ethics approval was not required for this research.

Author contribution

Débora Natalia López: Methodology (lead); Writing-original draft (lead). **Romina Ingrassia:** Methodology (supporting); Writing-original draft (supporting). **Pablo Busti:** Funding acquisition (supporting); Writing-review & editing (lead). **Jorge Ricardo Wagner:** Resources (lead); Writing-review & editing (supporting). **Valeria Boeris:** Funding acquisition (lead); Resources (supporting); Supervision (supporting); Writing-review & editing (lead). **Darío Spelzini:** Funding acquisition (supporting); Resources (supporting); Supervision (lead); Writing-review & editing (supporting).

Peer Review

The peer review history for this article is available at https://publons.com/publon/10.1111/ijfs.14784.

Data availability statement

Data available on request from the authors.

References

Alting, A.C., Hamer, R.J., Kruif, C.G.De & Visschers, R.W. (2000). Formation of disulfide bonds in acid-induced gels of preheated whey protein isolate. *Journal of Agricultural and Food Chemistry*, **48**, 5001–5007.

Alting, A.C., Hamer, R.J., de Kruif, C.G. & Visschers, R.W. (2003). Cold-set globular protein gels: interactions, structure and rheology as a function of protein concentration. *Journal of Agricultural and Food Chemistry*, **51**, 3150–3156.

Alting, A.C., Weijers, M., de Hoog, E.H.A. *et al.* (2004). Acid-induced cold gelation of globular proteins: Effects of protein aggregate characteristics and disulfide bonding on rheological properties. *Journal Agricultural Food Chemistry*, **52**, 623–631.

Cavallieri, A. & da Cunha, R.L. (2008). The effects of acidification rate, pH and ageing time on the acidic cold set gelation of whey proteins. *Food Hydrocolloids*, **22**, 439–448.

Chu, L., Yang, L., Li, J., Lin, L. & Zheng, G. (2019). Effect of *Smilax china* L. starch on the gel properties and interactions of calcium sulfate-induced soy protein isolate gel. *International Journal of Biological Macromolecules*, **135**, 127–132.

Cui, Q., Wang, X., Wang, G. *et al.* (2019). Effects of ultrasonic treatment on the gel properties of microbial transglutaminase crosslinked soy, whey and soy–whey proteins. *Food Science and Biotechnology*, **28**, 1455–1464.

Djoullah, A., Djemaoune, Y., Husson, F. & Surel, L. (2015). Native-state pea albumin and globulin behavior upon transglutaminase treatment. *Process Biochemistry*, **50**, 1284–1292.

Donato, L., Garnier, C., Novales, B., Durand, S. & Doublier, J.L. (2005). Heat-induced gelation of bovine serum albumin/low-methoxyl pectin systems and the effect of calcium ions. *Biomacromolecules*, **6**, 374–385.

Donato, L., Kolodziejcyk, E. & Rouvet, M. (2011). Mixtures of whey protein microgels and soluble aggregates as building blocks to control rheology and structure of acid induced cold-set gels. *Food Hydrocolloids*, **25**, 734–742.

Gharibzahedi, S.M.T. & Smith, B. (2020). The functional modification of legume proteins by ultrasonication: A review. *Trends in Food Science and Technology*, **98**, 107–116.

Hernández-Carrión, M., Hernando, I., Sotelo-Díaz, I., Quintanilla-Carvajal, M.X. & Quiles, A. (2015). Use of image analysis to evaluate the effect of high hydrostatic pressure and pasteurization as preservation treatments on the microstructure of red sweet pepper. *Innovative Food Science and Emerging Technologies*, **27**, 69–78.

Hidalgo, M.E., Fontana, M., Armendariz, M., Riquelme, B., Wagner, J.R. & Risso, P. (2015). Acid-induced aggregation and gelation of sodium caseinate-guar gum mixtures. *Food Biophysics*, **10**, 181–194.

Ingrassia, R., Palazolo, G., Wagner, J. & Risso, P. (2019). Heat treatments of defatted soy flour: Impact on protein structure, aggregation, and cold-set gelation properties. *Food Structure*, **22**, 100–130.

Jiang, S., Ding, J., Andrade, J. *et al.* (2017). Modifying the physicochemical properties of pea protein by pH-shifting and ultrasound combined treatments. *Ultrasonics Sonochemistry*, **38**, 835–842.

Kharlamova, A., Chassenieux, C. & Nicolai, T. (2018). Acid-induced gelation of whey protein aggregates: Kinetics, gel structure and rheological properties. *Food Hydroccoloids*, **81**, 263–272.

Li, X., Mao, L., He, X., Ma, P., Gao, Y. & Yuan, F. (2018). Characterization of β-lactoglobulin gels induced by high pressure processing. *Innovative Food Science and Emerging Technologies*, **47**, 335–345.

Liu, G., Buldo, P., Greve, M., Nielsen, S., Nielsen, J. & Ipsen, R. (2016). Effects of added whey protein aggregates on textural and microstructural properties of acidified milk model systems. *International Dairy Journal*, **62**, 43–52.

Lombardi, J., Pellegrino, J.M., Soazo, M. *et al.* (2018). Mineral fortification modifies physical and microstructural characteristics of milk gels coagulated by a bacterial enzymatic pool. *Colloids and Surfaces B: Biointerfaces*, **161**, 296–301.

López, D.N., Ingrassia, R., Busti, P., Wagner, J., Boeris, V. & Spelzini, D. (2018). Effects of extraction pH of chia protein isolates on functional properties. *LWT-Food Science and Technology*, **97**, 523–529.

Lu, H., Zhang, L., Li, Q. & Luo, Y. (2017). Comparison of gel properties and biochemical characteristics of myofibrillar protein from bighead carp (*Aristichthys nobilis*) affected by frozen storage and a hydroxyl radical-generation oxidizing system. *Food Chemistry*, **223**, 96–103.

Mäkinen, O.E., Zannini, E. & Arendt, E.K. (2015). Modifying the cold gelation properties of quinoa protein isolate: Influence of heat-denaturation pH in the alkaline range. *Plant Foods for Human Nutrition*, **70**, 250–256.

Mession, J.L., Chihi, M.L., Sok, N. & Saurel, R. (2015). Effect of globular pea proteins fractionation on their heat-induced aggregation and acid cold-set gelation. *Food Hydrocolloids*, **46**, 233–243.

Mir, N.A., Riar, C.S. & Singh, S. (2019). Structural modification of quinoa seed protein isolates (QPIs) by variable time sonification for improving its physicochemical and functional characteristics. *Ultrasonics Sonochemistry*, **58**, 104700.

Mishyna, M., Martinez, J.J.I., Chen, J., Davidovich-Pinhas, M. & Benjamin, O. (2019). Heat-induced aggregation and gelation of proteins from edible honey bee brood (*Apis mellifera*) as a function of temperature and pH. *Food Hydrocolloids*, **91**, 117–126.

Montellano Duran, N., Galante, M., Spelzini, D. & Boeris, V. (2018). The effect of carrageenan on the acid-induced aggregation and gelation conditions of quinoa proteins. *Food Research International*, **107**, 683–690.

Mortensen, A.B. & Wallin, H. (1989). Gravimetric determination of ash in foods: NMKL collaborative study. *Journal of AOAC INTERNATIONAL*, **72**, 481–483.

Özkan, N., Xin, H. & Chen, H. (2002). Application of a depth sensing indentation hardness test to evaluate the mechanical properties of food materials. *Journal of Food Science*, **67**, 1814–1820.

Prosky, L., Asp, N.-G., Furda, I., Devries, J.W., Schweizer, T.F. & Harland, B.F. (1985). Determination of total dietary fiber in foods and food products: collaborative study. *Journal of AOAC International*, **68**, 677–679.

Risso, P.H., Relling, V.M., Armesto, M.S., Pires, M.S. & Gatti, C.A. (2007). Effect of size, proteic composition, and heat treatment on the colloidal stability of proteolyzed bovine casein micelles. *Colloid and Polymer Science*, **285**, 809–817.

Shih, C., Chang, Y., Hsie, B. & Wu, J. (2013). Microscopic SEM texture analysis of NIPAM gel dosimeters. *IEEE Transactions of Nuclear Science*, **60**, 2155–2160.

Smith, P.K., Krohn, R.I., Hermanson, G.T. *et al.* (1985). Measurement of protein using bicinchoninic acid. *Analytical Biochemistry*, **150**, 76–85.

Soukoulis, C., Cambier, S., Serchi, T. *et al.* (2019). Rheological and structural characterisation of whey protein acid gels co-structured

with chia (*Salvia hispanica* L.) or flax seed (*Linum usitatissimum* L.) mucilage. *Food Hydrocolloids*, **89**, 542–553.

Supporting Information

Additional Supporting Information may be found in the online version of this article:

Table S1. Physicochemical characterization of CPI10, CPI12 and their heat-treated dispersions.

Table S2. Characterization of the acid-induced gelation of CPI10 and CPI12.

Table S3. Digital analysis of micrographs from CPI10 and CPI12 acidified systems.